Journal of Photochemistry and Photobiology A: Chemistry 204 (2009) 129–136

Contents lists available at ScienceDirect

Journal of Photochemistry and Photobiology A: Chemistry

journal homepage: www.elsevier.com/locate/jphotochem

Photoelectrocatalytic degradation of the insecticide imidacloprid using TiO_2/Ti electrodes

N. Philippidis [a], S. Sotiropoulos [a], A. Efstathiou [b], I. Poulios [a,*]

[a] Lab. Physical Chemistry, Department of Chemistry, Aristotle University of Thessaloniki, University Campus, Thessaloniki 54124, Macedonia, Greece
[b] Department of Chemistry, Heterogeneous Catalysis Laboratory, University of Cyprus, P.O. Box 20537, Nicosia CY 1678, Cyprus

ARTICLE INFO

Article history:
Received 1 December 2008
Received in revised form 12 February 2009
Accepted 10 March 2009
Available online 21 March 2009

Keywords:
Photoelectrocatalysis
TiO_2
Imidacloprid
Pesticides

ABSTRACT

The photoelectrocatalytic degradation and mineralization of the chlorinated nicotinoid insecticide imidacloprid in aqueous solution has been investigated. Experiments were carried out using as working electrodes TiO_2 P-25 coatings, prepared by the dip coating method, on Ti substrates (TiO_2/Ti). After annealing at 500 °C for 1.5 h, the surface morphology of the TiO_2 film electrodes was examined by scanning electronic microscopy (SEM) and X-ray diffraction (XRD). From capacity measurements the flat band potential has been calculated (V_{fb} = −0.54 V vs Ag/AgCl, pH = 5.6), as well as the donor density of the deposited TiO_2 film electrodes. Photocurrents vs applied potential curves was used for their preliminary photoelectrochemical characterization. The photoelectrocatalytic efficiency (PEC) of the TiO_2/Ti electrodes, concerning the imidacloprid oxidation has been evaluated in terms of degradation and mineralization under various experimental conditions. The selected pollutant was effectively degraded following the first order kinetics model. The degradation efficiency increased with increasing of applied potential bias up to +1.5 V vs Ag/AgCl and is more favourable in acidic than in alkaline environments. The results of the photoelectrocatalytic experiments were compared to those of photochemical and photocatalytic (PC) degradation of the insecticide and showed a significant synergy effect in the case of the PEC degradation, leading at +1.5 V to an 249% increase of the apparent rate constant, k_o, in comparison to the simple photocatalytic process.

1. Introduction

In the beginning of the 21st century, the domestic and the industrial/agricultural activity, especially in the developed countries, generate high amounts of residual wastewater, whose direct disposal to natural channels has a considerable effect on the environment. This fact, together with the need to restore these water resources for new uses, makes essential the purification of wastewater to achieve the desired degree of quality.

Due to an increasing social and political concern for the environment, the research field of water purification has been extensively growing in the last decades, comprising both polluted wastewaters and groundwaters from seas, rivers and lakes, as water quality control and regulations against hazardous pollutants have become stricter in many countries. More recently, reflecting a new environmental conscience, the European Directive 2000/60/CE [1] stresses the need to adopt measures against water pollution in order to achieve a progressive reduction of pollutants.

Facing the fact that many toxic organic compounds are designed to be chemically stable, a number of "traditional methods", such as chlorination, ozonolysis, carbon adsorption and air stripping, are being used to solve the problem. Unfortunately, these methods tend to have several problems associated with them, e.g. the use of toxic reagents in chlorination and ozonolysis [2,3] and the transfer of the pollution problem from one phase to another in the case of carbon adsorption and air stripping [4]. On the other hand, a group of alternative methods, the so-called advanced oxidation processes (AOPs) appear to be promising in the abatement of the growing environmental problems resulting from these toxic compounds, as they can provide almost total degradation [5,6].

The use of semiconductor photocatalysts in the presence of artificial or solar light has been growing steadily over the last 20 years, because they offer a simple and cheap process for destroying organic compounds [7–10]. The photocatalyst which has received most attention in recent years is titanium dioxide (TiO_2) due to its chemical stability against corrosion and photocorrosion and its reasonable photocatalytic activity, especially when used in its anatase form. TiO_2 is usually used as slurry of fine particles in a photochemical reactor. This approach has the advantage of relative high purification efficiency, since the slurry may provide a high photoinduced reaction surface. However, the ultimate separation of the

* Corresponding author. Tel.: +30 2310997785; fax: +30 2310997784.
E-mail address: poulios@chem.auth.gr (I. Poulios).

1010-6030/$ – see front matter © 2009 Elsevier B.V. All rights reserved.
doi:10.1016/j.jphotochem.2009.03.007

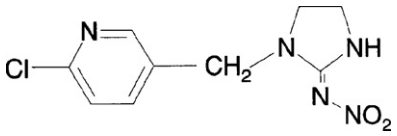

Fig. 1. Chemical structure of the insecticide imidacloprid, CAS 138261-41-3.

TiO_2 particulates from the treated wastewater is very difficult. Any approach of TiO_2 separation may result in high operation expenses and complex treatment system. Immobilizing the TiO_2 particles onto supporting materials avoids the separation step, although a decrease of quantum efficiency is then observed, due to the diffusion limitations of the organic substance to the catalyst and the decrease in its surface area. Many efforts have been made to solve this problem [11,12]. Among them, TiO_2 was supported on an electronic conductor and biased positive with the application of an external voltage in an appropriate photoelectrochemical cell, so that the rate of the photogenerated electron–hole recombination is limited and the rate of the surface reactions increased (photoelectrocatalytic oxidation) [13–17].

The aim of the present work was the preparation of TiO_2 coatings on Ti substrates using the dip coating method, their characterization and the study of their photoelectrocatalytic activity towards the degradation of the insecticide imidacloprid in a novel photoelectrochemical reactor.

Imidacloprid (Fig. 1) belongs to a new class of insecticides, called neonicotinoids. Since its launch in 1991, products containing imidacloprid have gained registrations in about 120 countries and are marketed for use in agriculture (for over 140 agricultural crops), on turf, pets and for household pests [18]. The chemical works by interfering with the transmission of stimuli in the insect nervous system. It is very toxic to earth worms and bees and is restricted in France because of plummeting bee populations. Specifically, it causes a blockage in a type of neuronal pathway (nicotinergic) that is more abundant in insects than in warm-blooded animals. Although no evidence of human poisoning was found in the literature, signs and symptoms of poisoning would be expected to be similar to nicotinic signs and symptoms, including fatigue, twitching, cramps, and muscle weakness including the muscles necessary for breathing [19].

2. Experimental details

2.1. Chemicals

Imidacloprid, $C_9H_{10}O_2N_5Cl$, 1-[(6-chloro-3-pyridinyl)methyl]-N-nitro-2-imidazolidinimine, technical grade (99% purity), was purchased from the company PharmaChem, Thessaloniki, Greece. The TiO_2 used throughout this work was from Degussa Huells (TiO_2 P-25 Degussa, anatase/rutile: 3.6/1, surface area 56 $m^2\,g^{-1}$, nonporous). H_2SO_4 and NaOH used to adjust the pH when necessary, as well as anhydrous Na_2SO_4 (p.a. >99%) was from Merck. Ti plates (0.5 mm thick) were from Alfa Aesar (99.5%, metals basis). Doubly distilled water was used throughout the work. Aqueous stock solutions of imidacloprid (200 mg L^{-1}) were prepared every week, protected from light and stored at 25 °C.

2.2. Analytical methods

Scanning electron microscopy (SEM) was carried out using a JSM 733 microscope. X-ray diffraction (XRD) coating characterization was performed with a SHIMADZU X-ray diffractometer (Lab X, XRD-6000). The rutile content in the TiO_2 electrodes after annealing was calculated according to the following expression [20], $x = 1 + 0.8-$, where x is the weight fraction of rutile in the powder and I_A and I_R are the intensities of the characteristic peaks of anatase and rutile, respectively.

Absorption spectra in the ultraviolet and visible range were recorded with a Shimadzu PharmaSpec UV-100 spectrophotometer, while for the differential capacity measurements a PGZ301 Voltalab 40 electrochemical system from Dynamic Electrochemical Laboratory was used. A total organic carbon analyzer (Shimadzu Instruments, model TOC-V_{CSH}) was used to monitor the dissolved organic carbon (DOC) reduction. During the degradation experiments, samples of 4 ml for the absorption spectra and 6 ml for the DOC analysis were withdrawn from the reactor at the desired time intervals.

2.3. TiO_2/Ti electrode preparation

Ti specimens of geometric surface area 0.5 cm^2 for the characterization of the electrodes or Ti cylindrical foils of geometric surface area 220 cm^2 (10 cm × 22 cm) for the bulk photoelectrocatalytic experiments, were cut from 0.5 mm thick Ti plates and were etched for a few seconds in a HF/HNO_3 3:1 mixture before washed thoroughly with doubly distilled water. The procedure was repeated several times. The deposition of TiO_2 P-25 onto the Ti substrate took place from a 4 g L^{-1} TiO_2 suspension by a dip coating, drying and sintering procedure. Briefly, 2 g TiO_2 was added to 500 ml methanol, sonicated for 30 min to break up loosely attached aggregates and then vigorously agitated to form a fine TiO_2 suspension. The dip coating was done manually by immersing the substrates in the precursor solution for about 2 s. The TiO_2/Ti specimens were dried for 7 min in a muffle furnace at 80 °C in order the methanol to be evaporated. This process was repeated as required to produce TiO_2 films with a loading of 1 mg cm^{-2}, which corresponds to a 6.5 μm thickness. Finally the working electrodes were prepared by annealing the particulate TiO_2/Ti specimens in air at 500 °C for 1.5 h, in a Carbolite CWF 1100 oven, in order to improve the crystallinity and the adhesion of the prepared films. To study the effect of temperature in the range of 400–600 °C similar procedures were adopted, leading to films which show a lower photoelectrocatalytic activity in comparison to the respective one calcinated at 500 °C. Finally, locations on the back side of the electrodes were etched again (to remove oxides formed by annealing) and insulated Cu wire was glued onto them with a silver epoxy resign. The contact, as well as the entire back side of the electrodes, were insulated with epoxy resign glue in order to eliminate its contribution to the dark current.

2.4. Experimental setup and procedures

For the electrochemical/photoelectrochemical characterization of the produced TiO_2 films a classical three compartment photoelectrochemical cell was employed. The electrolyte volume in each compartment was 12 ml. The anodic compartment contained the working electrode and a Ag/AgCl electrode as reference, while the cathodic compartment held a platinum wire as counter electrode. Voltammograms were run for at least three times, since preliminary experiments showed that steady state conditions were observed after the third run. An Osram Dulux 9W/78 UVA lamp (A = 320–400 nm, A_{max} = 365 nm) was placed at a distance of 3 cm from the working electrode and was used as the illumination source. For the electrochemical measurements in the dark and under illumination the computer controlled electrochemical system DUO 18 (World Precision Instruments) was used.

The electrochemical reactor for the bulk photoelectrolysis experiments is shown in Fig. 2. It consisted of a 500 cm^3 cylindrical cell (i.d. = 7.8 cm; height = 14.8 cm) with a removable cap and inlet and outlet ports for sparging the desired gas. The same Osram Dulux 9W/78 UVA lamp was placed in a cylindrical borosilicate glass sleeve, and introduced in the middle of the reactor. The light

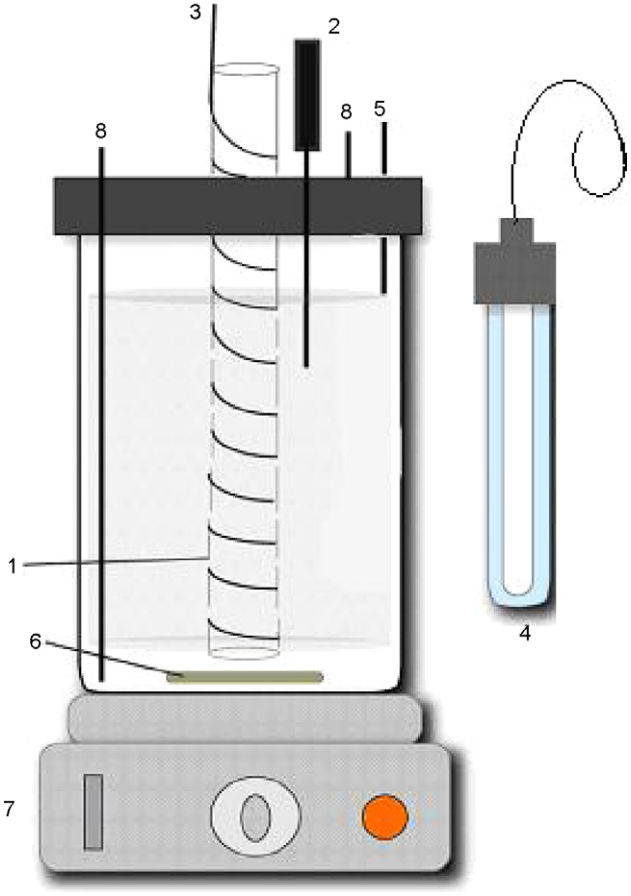

Fig. 2. Schematic representation of the photoelectrocatalytic reactor: (1) cylindrical sleeve where lamp (4) is inserted; (2) Ag/AgCl reference electrode; (3) counter electrode (stainless steel wire); (4) UVA lamp; (5) working electrode (TiO_2/Ti cylinder); (6) magnet; (7) magnetic stirrer; (8) inlet and outlet ports.

intensity on the TiO_2 electrode surface position was measured as 3.9 mW cm^{-2} with a photometer (Solar Light Co. PMA 2100), while the flux of the UV-A photons emitted into the 340 cm^3 reaction solution was found to be 2.1×10^{-6} einstein L^{-1} s^{-1} by ferrioxalate actinometry [21]. The TiO_2/Ti electrode of 220 cm^2 surface area was fitted between the cylindrical sleeve and the inner wall of the cell. A stainless steel wire was coiled around the sleeve and was used as counter electrode, while a Ag/AgCl electrode equipped with a salt bridge made of a thin thermoplastic tube ending to a Vycor® tip was used as reference electrode. The applied potential was obtained using the potentiostat Wenking POS 73 (Bank Elektronik). The photoelectrochemical reactor was placed in a dark chamber in order to avoiding interferences from the daylight. All experiments were carried out at a temperature of 25 °C.

Some photocatalytic experiments were repeated three times in order to check the reproducibility of the experimental results. The reproducibility of the optical density values was within ±5%, while that of DOC ±10%.

3. Results and discussion

3.1. Characterization of the TiO_2/Ti electrodes

The XRD pattern of the TiO_2/Ti electrode annealed at 500 °C for 1.5 h is shown in Fig. 3. A high intensity signal for anatase TiO_2 (at $2\theta = 25.28°$) was found, while a weak peak from the rutile phase appeared at $2\theta = 28.06°$. Thus, the anatase form of TiO_2 was dominant in the TiO_2/Ti film, in accordance with the specification of the starting Degussa P-25 material.

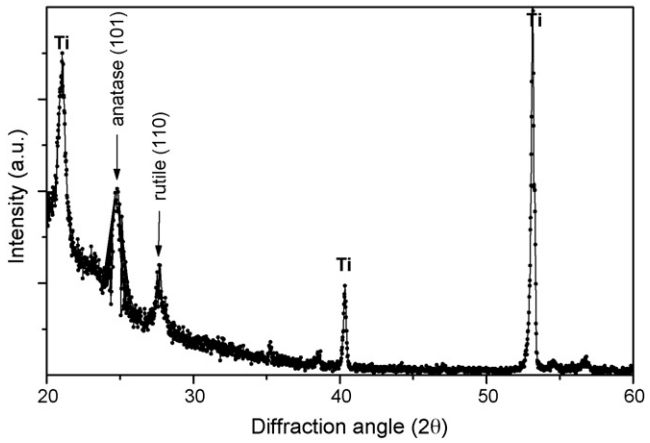

Fig. 3. XRD diffractogram of the TiO_2/Ti specimen after 1.5 h annealing at 500 °C.

Fig. 4 on the other hand depicts the surface morphology of the particulate TiO_2/Ti working electrode, characterized by a network of spherical few micrometer-sized aggregates into which the few tens of nanometer P-25 particles (ca. 30 nm, as confirmed by XRD peak analysis) have merged, following annealing at 500 °C for 1.5 h.

3.2. Electrochemical/photoelectrochemical characterization of the TiO_2/Ti electrodes

The electrochemical behavior of many semiconductor materials has been interpreted in terms of Schottky barrier behavior, in the theoretical framework of solid state metal–semiconductor Schottky junctions [22,23]. In the simplest case, the classical Mott–Schottky relationship can be used to calculate two important parameters related to the electronic properties of the tested material, namely the flat band potential (V_{fb}) and the donor density (N_D), in the case of n-type semiconductors, according to Eq. (1)

$$\frac{1}{C^2} = \frac{2}{\varepsilon\varepsilon_o e N_D}\left(V - V_{fb} - \frac{kT}{e}\right) \quad (1)$$

where ε is the average value of the semiconductor dielectric constant (~120 for TiO_2 [24]), ε_o the permittivity of the free space charge, N_D the donor density and e the absolute value of the electron charge. V corresponds to the external applied potential, while T and k are the absolute temperature and the Boltzmann constant, respectively.

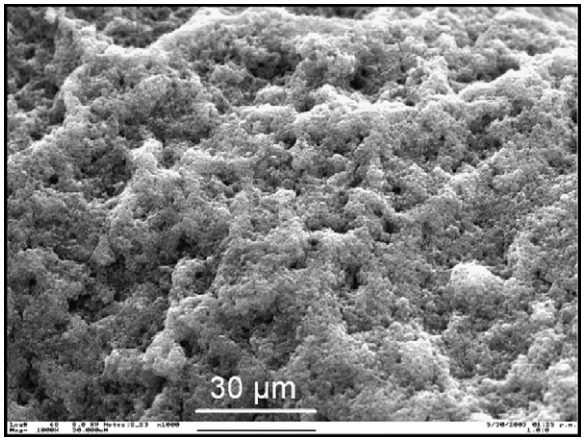

Fig. 4. SEM image of the particulate TiO_2/Ti specimen after annealing at 500 °C for 1.5 h.

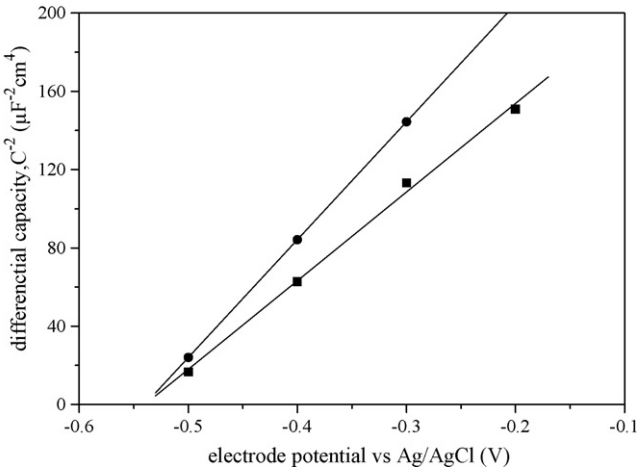

Fig. 5. Mott–Schottky plot of the TiO_2/Ti electrode in 0.1 M Na_2SO_4 in the dark at (■) 100 Hz and (●) 500 Hz (initial pH = 5.6).

Fig. 5 presents the Mott–Schottky plot for a TiO_2/0.1 M Na_2SO_4 (pH = 5.6) electrochemical junction in the dark at 100 and 500 Hz. It can be seen that in both frequencies, for an appreciably wide potential range, the C^{-2} vs V plots show good linearity. From the intercept of these lines with the potential axis and according to Eq. (1) a value of – 0.540 V vs Ag/AgCl or – 0.318 V vs the normal hydrogen electrode (NHE) at pH = 5.6, for the V_{fb} of the semiconductor electrode has been calculated, while the donor density, N_D, calculated from the slope of the line, which corresponds to the frequency of 100 Hz, according Eq. (1) is 3.2×10^{18} cm^{-3}. These experimental values are in good agreement with values reported in the literature [25] and the n-type behavior of the deposited films is also confirmed.

The current–potential curve of the particulate TiO_2/Ti electrode in a 0.1 M Na_2SO_4 aqueous solution, under dark conditions and under UV-A illumination, recorded within the potential range of −0.8 and +2 V vs Ag/AgCl at a potential sweep rate of 10 mV s^{-1} is given in Fig. 6. The value of the photocurrent density, as well as the overall photoelectrochemical efficiency of a TiO_2 electrode depends on various factors, such as preparation method and procedure, heat treatment conditions etc. In our case, by using the dip coating method, the best results, concerning the photoelectrocatalytic efficiency, for specimens treated between 400 and 700 °C and for time intervals 1.5 until 10 h, were obtained with electrodes annealed at 500 °C for 1.5 h. For this reason all bulk photoelectrocatalytic experiments, concerning the imidacloprid degradation, were carried out by using these electrodes.

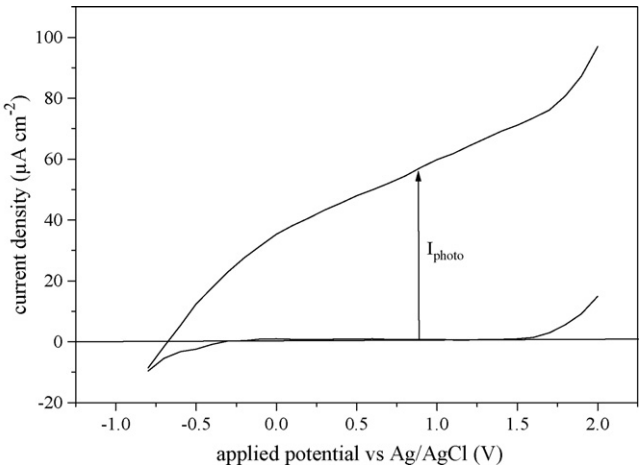

Fig. 6. Linear sweep voltammogram (LSV) for TiO_2/Ti in 0.1 M Na_2SO_4, in the dark and under illumination. Sweep rate 10 mV s^{-1}, pH = 5.6.

As can be seen in Fig. 6 the particulate TiO_2/Ti electrode shows in the potential range of −0.5 to +1.6 V nearly perfect blocking characteristics, while an increase in dark current density for potentials higher than +1.6 V has been observed as a result of the water decomposition and the oxygen evolution. At potentials more negative than −0.5 V, both a cathodic peak and an ill-defined anodic hump or peak are observed (not shown in the figure), the former corresponding to the reduction of surface Ti(IV) species and the latter to the re-oxidation of surface Ti(III) species [27].

On the contrary, upon illumination a significant increase in the anodic current density above −0.5 V vs Ag/AgCl occurred. According to the literature [22,25,26,28,29], by illuminating a semiconductor–electrolyte interface with light energy greater than that of its band gap energy, electron–hole pairs are generated at the electrode surface. The simultaneous application of a bias potential positive to the flat band potential produces a bending of the conduction and valence band causing a more effective separation of the photogenerated carriers within the space charge layer and increases the photocurrent (I_{photo}) that begins to flow and likely promotes better the oxidative degradation process. The potential gradient efficiently force the electrons to arrive at the counter electrode and leave the photogenerated holes to react with H_2O/OH^- to give rise to OH• radicals or to react directly with the organics presented in the solution.

3.3. Bulk photoelectrocatalytic oxidation of imidacloprid at the TiO_2/Ti electrodes

Fig. 7 shows the change in the absorption spectrum of 20 mg L^{-1} (7.82×10^{-5} M) imidacloprid during its photoelectrocatalytic degradation at an anodic bias of +1.5 V vs Ag/AgCl in a 0.1 M Na_2SO_4 solution. The absorption maximum at 270 nm is seen to decrease in intensity with increasing illumination time, vanishing almost completely within ~4 h. The disappearance of the absorption peak with reaction time indicates the complete decomposition of the imidacloprid molecule.

The synergistic effect of the applied potential on the photocatalytic process during the degradation of imidacloprid in a 0.1 M Na_2SO_4 solution can be seen in Fig. 8. Fig. 8A shows the performance

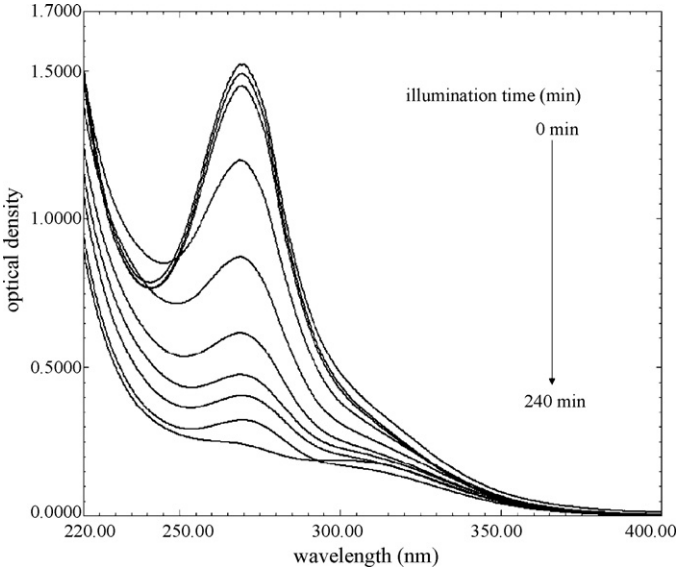

Fig. 7. UV–vis absorption spectra of 20 mg L^{-1} imidacloprid in 0.1 M Na_2SO_4 at pH = 5.6 during the photoelectrocatalytic degradation at different reaction times on the TiO_2/Ti particulate electrode biased at +1.5 V vs Ag/AgCl.

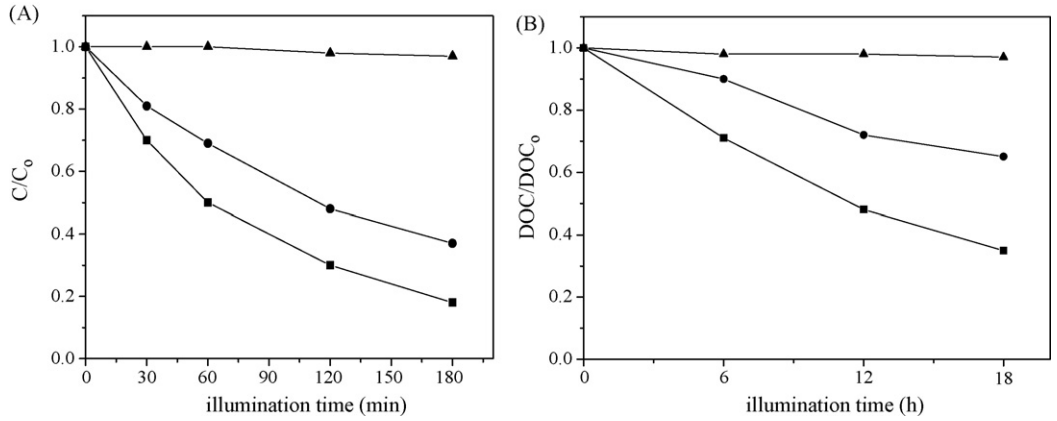

Fig. 8. Degradation (A) and mineralization (B) of imidacloprid on a TiO_2/Ti electrode as a function of illumination time: (▲) photolytic oxidation (●) photocatalytic oxidation without applied potential and (■) photoelectrocatalytic oxidation in the presence of UV-A light and V = +1.5 V vs Ag/AgCl. In all cases, the imidacloprid concentration was 20 mg L^{-1} in 0.1 M Na_2SO_4 and pH = 5.6.

of the TiO_2/Ti particulate electrode, under various experimental conditions, with respect to the decrease of the insecticide's concentration as a function of the illumination time. The relative decrease of the insecticide's concentration is the ratio of the insecticide's concentration at time t to its initial one in the solution at t = 0. Three distinct sets of conditions were investigated: (a) the photolytic degradation in the absence of the catalyst, (b) the photocatalytic degradation efficiency by using UV-A light without an applied potential and finally (c) the photoelectrocatalytic degradation, i.e. using both UV-A light and a +1.5 V bias potential. As indicated in Fig. 8A and in Table 1, where the apparent first order reaction rate constants of degradation (k_o) under the different experimental conditions are given, the photolytic oxidation contributed less than 5% to the degradation of imidacloprid after 3 h of reaction time, while the pure photocatalytic process (without applying potential, corresponding to the open circuit conditions) leads after 3 h of illumination to a 63% decrease of the imidacloprid concentration. However, when applying an anodic potential of +1.5 V, the photodegradation efficiency was increased to 82%, showing that the applied potential increases significantly the degradation rate of the insecticide.

The photodecomposition of imidacloprid, like other organic pollutants, is a complicated process with a lot of intermediate products. These intermediates are of great significance in water treatment, because they can be proved more toxic than the parent compounds. Thus, it is of vital importance to succeed complete mineralization of the organic pollutants via the photoelectrocatalytic method.

Fig. 8B shows the extent of the DOC reduction vs illumination time of a solution containing 20 mg L^{-1} imidacloprid, while in Table 1 the apparent reaction rate constants of the mineralization (k_{DOC}) of the pesticide under the same experimental conditions as in Fig. 8A are given. The photoelectrocatalytic oxidation at +1.5 V leads to a 66% reduction of the initial carbon content of imidacloprid after 18 h of illumination, while at the same time (see Fig. 8A) the decomposition was almost complete, showing the presence of difficult to degradate intermediates. In the case of the simple photocatalytic oxidation, as in the degradation results, the photomineralization proceeds with lower efficiency compared to the one when an anodic potential has been applied and at the same reaction time only 36% of the initial organic content contained in the imidacloprid molecule is converted to CO_2. The photolytic oxidation on the other hand, under the given experimental conditions, seems to be a very insufficient process concerning the destruction, as well as the mineralization of the insecticide.

Table 1
Apparent rate constants of degradation, k_o and mineralization, k_{DOC}, of 20 mg L^{-1} imidacloprid in a 0.1 M Na_2SO_4 solution under various experimental conditions.

Experimental conditions	Apparent rate constant of degradation, $k_o \times 10^4$ (s^{-1})	Apparent rate constant of mineralization, $k_{DOC} \times 10^5$ (s^{-1})
Photoelectrocatalytic, pH = 5.6, +1.5 V vs Ag/AgCl	1.56 ± 0.06	1.70 ± 0.07
Photoelectrocatalytic, pH = 3, +1.5 V vs Ag/AgCl	2.27 ± 0.16	1.54 ± 0.04
Photoelectrocatalytic, pH = 9, +1.5 V vs Ag/AgCl	0.42 ± 0.03	1.71 ± 0.10
Photocatalytic, pH = 5.6	0.92 ± 0.04	0.73 ± 0.07
Photochemical, pH = 5.6, +1.5 V vs Ag/AgCl	0.04 ± 0.003	0.09 ± 0.005

These results illustrate that the insecticide degradation by photoelectrocatalytic procedures is more effective than the pure photochemical or photocatalytic one. As already stated, the application of the positive potential bias to the TiO_2/Ti electrolyte interface provides a potential gradient within the semiconductor layer, which is able to drive the photogenerated holes and electrons efficiently apart. As a result, the charge recombination of the photogenerated carriers is reduced, and consequently, larger number of positively charged holes are available for the photooxidation of H_2O or the imidacloprid molecule and the various intermediate products, which are adsorbed onto the TiO_2 surface.

The rate of the photoelectrocatalytic degradation of imidacloprid at the TiO_2/Ti electrode is sensitive to different factors, such as the applied potential, the initial concentration of the imidacloprid molecule and pH, the light intensity, etc. and some of these parameters are discussed subsequently below.

The photocatalytic degradation rate of organic compounds is commonly described by a pseudo-first order kinetic expression, which is rationalized in terms of the Langmuir–Hinshelwood (L–H) model, modified to accommodate reactions occurring at the solid–liquid interface [30,31].

$$r_o = -\frac{dC}{dt} = \frac{k_r K C}{1 + KC} \quad (2)$$

where r_o is the initial rate of disappearance of the organic substrate and C is the initial bulk-solute concentration. K represents the equilibrium constant of adsorption of the organic substrate onto TiO_2 and k_r reflects the limiting rate constant of reaction at maximum coverage under the given experimental conditions. This equation can be used when data exhibit sufficient linearity, when plotted as follows:

$$\frac{C}{r_o} = \frac{1}{k_r K} + \frac{C}{k_r} \quad (3)$$

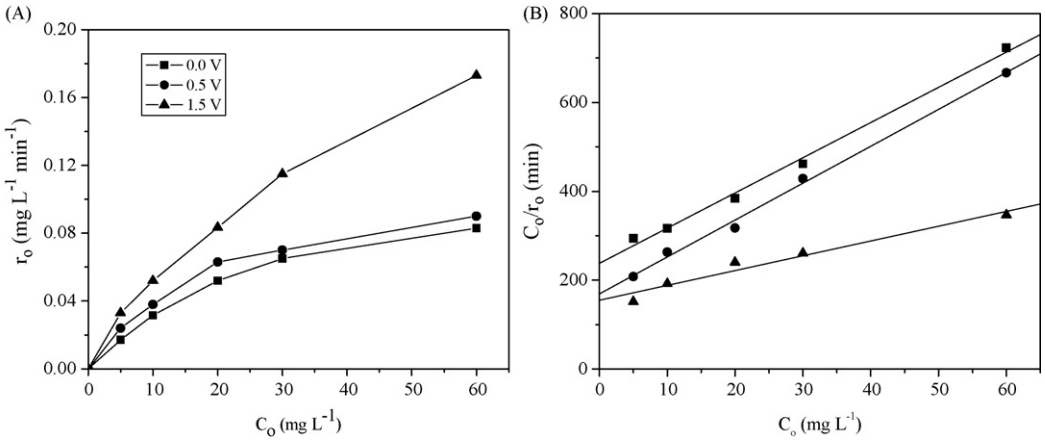

Fig. 9. (A) Plot of r_o vs C, at various initial concentrations of imidacloprid from 5 to 50 mg L^{-1} for (■) 0 V, (●) 0.5 V and (▲) 1.5 V vs Ag/AgCl. (B) Linear transform of C/r_o vs C according to Eq. (3).

The effect of altering the initial concentration of imidacloprid on the initial reaction rate (r_o) of photodegradation in three different anodic potential values is shown in Fig. 9A.

The r_o values were independently obtained by a linear fit of the C–t data in the range of 5–50 mg L^{-1} (1.95–19.5 × 10^{-5} M) initial imidacloprid concentration. Only the experimental data obtained during the first 60 min illumination were used in calculating the initial reaction rates, in order to minimize variations as a result of the competitive effects of the intermediates, pH changes, etc. It is well known that the intermediate products formed during the photodegradation furthermore undergo photoelectrocatalytic oxidation, while the simultaneous release of H^+ influences the pH of the solution, thus resulting in a change of the initial conditions. The curves are reminiscent of a Langmuir type isotherm, at which the rate of decomposition first increases and then reaches a saturation value at high concentrations of imidacloprid, showing that the degradation depends also on other parameters, such as the rate of the charge or the mass transfer on the electrode double layer. In Fig. 9A it can be seen the positive effect of the applied voltage on the apparent rate constant. The greatest increase in degradation rate was observed for the bias voltage of +1.5 V. This is consistent with the observed increase in photocurrent between −0.5 and +1.5 V vs Ag/AgCl (Fig. 6).

The dependence of C/r_o values on the respective initial concentrations of imidacloprid for the three different applied potentials is shown in Fig. 8B. From the slope and the intercept of the resulting straight lines according to Eq. (3), the respective k_r and K values are calculated. As already mentioned K represents the equilibrium constant for the adsorption of imidacloprid onto TiO_2 and k_r reflects the limiting rate of reaction at maximum coverage for the given experimental conditions and accordingly have no absolute meaning.

For low initial solute concentrations, as in our case, Eq. (2) can be converted, after integration, to the pseudo-first order kinetic Eq. (4),

$$\ln \frac{C_0}{C} = k_o t \tag{4}$$

with an apparent rate constant k_o expressed as $k_o = Kk_r$. The k_o values are calculated and plotted in Fig. 10 as function of the applied potential. As can be seen, in the concentration range between 5 and 50 mg L^{-1} (1.95–19.5 × 10^{-5} M), the kinetic constant of degradation (k_o) was only 5.2 × 10^{-4} s^{-1} at −0.3 V cell voltage (closer to the flatband potential) and increased up to 7 × 10^{-4}, 9.7 × 10^{-4} and 10.83 × 10^{-4} s^{-1} at 0, 0.5 and 1.5 V cell voltage respectively. In more details, applying +1.5 V, the kinetic constant (k_o) increased 155% and 112% compared to 0 and 0.5 V cell voltage respectively, while a 249% increase in k_o is achieved in comparison to the simple photocatalytic process. This means that the applied potential is a key parameter for the photoelectrocatalytic oxidation.

As the potential increases up to +1.5 V the rate of oxidation of imidacloprid increases, while further increasing the potential beyond this value does not improve the degradation rate. The potential at which the maximum rate of degradation is achieved depends on the conditions employed in synthesizing the photoelectrode but appears to be, according to the literature, no higher than +2 V. If the potential exceeds this value direct electrooxidation of H_2O or imidacloprid begins to occur [32].

3.4. The effect of pH on the degradation of imidacloprid

The solution pH affects the speciation of both the surface functional groups of the TiO_2/Ti electrode and the chemical forms of organic compounds in the solution [33,34]. The solution pH also affects the flat band potential, raising this at 59 mV per pH unit to the cathodic direction [35], thus lowering the oxidative power of the photogenerated holes. All of these pH dependent factors may affect the photoelectrocatalytic oxidation of an organic pollutant at the TiO_2 electrode.

Fig. 11 shows the effect of the initial solution pH on the degradation (A), as well as the mineralization (B) of 20 mg L^{-1} imidacloprid. All the experiments were conducted with an applied potential

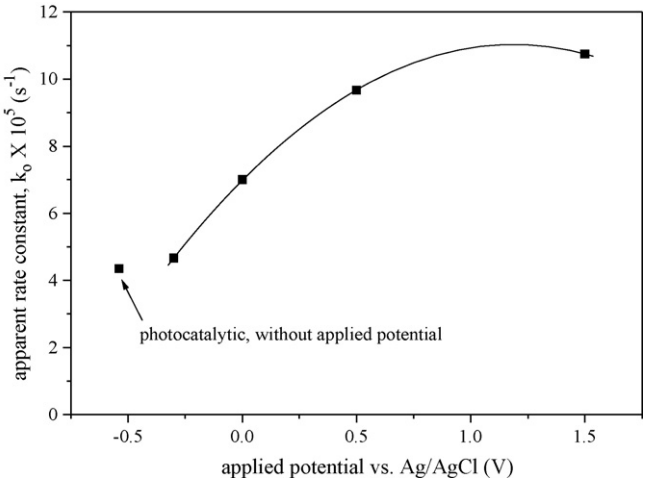

Fig. 10. Apparent rate constant k_o of the photoelectrocatalytic degradation of 20 mg L^{-1} imidacloprid in 0.1 M Na_2SO_4 as a function of the applied potential.

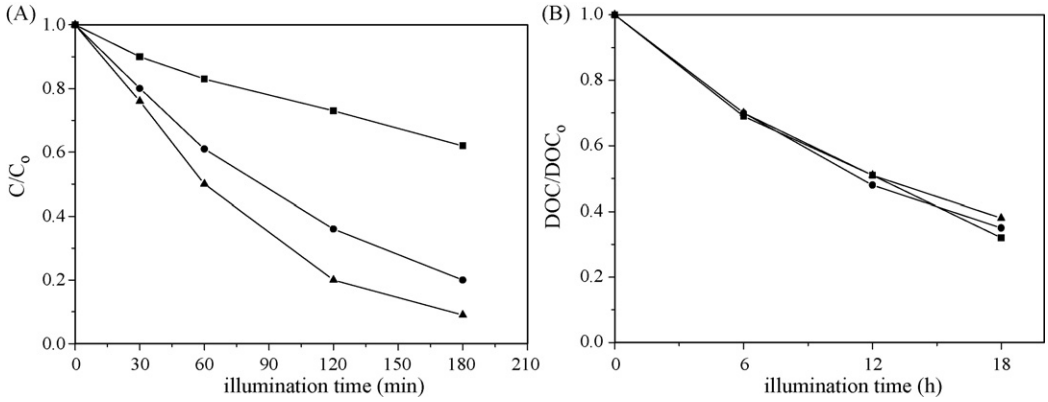

Fig. 11. Degradation (A) and mineralization (B) of imidacloprid on a TiO_2/Ti electrode as a function of illumination time at different initial pH values: (●) pH = 3, (■) pH = 5.6, (▲) pH = 9. In all cases, the imidacloprid concentration was 20 mg L^{-1} in 0.1 M Na_2SO_4.

across the photoanode/electrolyte interface of +1.5 V and a supporting electrolyte concentration of 0.1 M. Concerning the imidacloprid degradation, the experiments demonstrate, as can be seen in Fig. 11A and in Table 1, that a decrease on the destruction rate constant was observed when the pH was increased from 3 to 5.6 (natural pH) and 9. This observation is consistent with Yang's results concerning pentachlorophenol degradation [36], as well as with Kim and Anderson's results [37], where the maximum photoelectrocatalytic degradation of HCOOH occurred at pH = 3.4.

The mineralization process on the other hand seems to be independent from the initial pH value. This behavior could be explained as a result of the long reaction time leading to similar behavior in all cases. It has been observed that when starting with an initial pH of 5.6 or 9, its value decreases during the photodegradation until it reaches a minimum between 3.5 and 5, as a result of the mineralization and the production of the mineral acids.

4. Conclusions

In this work, the photoelectrocatalytic oxidative degradation of the insecticide imidacloprid, has been studied under artificial illumination in a novel photoelectrocatalytic reactor. It is observed that the particulate TiO_2/Ti electrode could be efficient with respect to degradation, as well as mineralization, although for practical achievement more active electrodes are needed. The degradation efficiency is faster by photoelectrocatalysis than by photocatalysis or by photochemical oxidation alone. This result indicates that there is a synergetic effect on degradation of imidacloprid when an appropriate irradiation and a potential difference are applied simultaneously on the particulate TiO_2/Ti electrode, leading to an 249% increase of the reaction rate constant in comparison to the simple photocatalytic process.

The photooxidation of 20 mg L^{-1} imidacloprid followed first order kinetics according to the Langmuir–Hinshelwood model, while parameters such as pH, applied potential and concentration of the insecticide play an important role affecting the reaction rate constant. Under the given experimental conditions the photoelectrocatalytic degradation of imidacloprid was found to be optimal when using +1.5 V vs Ag/AgCl cell voltage and a solution pH value equal to 3.

From the results of the present work and the respective literature one could claim that the photoelectrocatalytic oxidation could be employed as a powerful tool for the destruction of hazardous organics in water. The use of a low cost and chemical stable catalyst such as TiO_2 and the possibility of activating it with solar light, can offer economically reasonable and practical solutions to the processing of mixed wastes containing organics, as well as dissolved salts.

Acknowledgements

This work was supported by a Greek-Cyprus bilateral research program funded by the Greek General Secretariat of Research and Technology (GSRT) and NATO SFP 982835 project. The authors are indebted to Dr E. Paulidou, Department of Physics, Aristotle University of Thessaloniki for SEM micrographs.

References

[1] EC Directive 2000/60/EC of the European Parliament and of the Council of October 23, 2000 establishing a framework for community action in the field of water policy (L 327 of 22-12-2000).
[2] J.M. Symons, Am. Water Works Assoc. 67 (1975) 168.
[3] P.D. Foley, G.A. Missingham, Am. Water Work Assoc. 68 (1976) 105.
[4] J.W. Patterson, Industrial Wastewater Treatment Technology, 2nd ed., Butterworth, Boston, 1985.
[5] R. Andreozzi, V. Caprio, A. Insola, R. Martota, Catal. Today 53 (1999) 51–59.
[6] M. Litter, Introduction to photochemical advanced oxidation processes for water treatment, Environ. Chem. 2 (2005) 325–366.
[7] D. Blake, Bibliographic work on the heterogeneous photocatalytic removal of hazardous compounds from water and air, National Renewable Energy Laboratory, Technical Report, NREL/TP-510-31319, 2001.
[8] N. Sobana, M. Swaminathan, Sol Energy Mater. Sol Cells 91 (2007) 727–734.
[9] J. Nishio, M. Tokumura, H.T. Znad, Y. Kawase, J. Hazard. Mater. 138 (2006) 106–115.
[10] W. Baran, E. Adamek, A. Makowski, Chem. Eng. J. 145 (2008) 242–248.
[11] D.S. Tsoukleris, A.I. Kontos, P. Aloupogiannis, P. Falaras, Catal. Today 124 (2007) 110–117.
[12] E. Yassıtepe, H.C. Yatmaz, C. Öztürk, K. Öztürk, C. Duran, J. Photochem. Photobiol. A: Chem. 198 (2008) 1–6.
[13] K. Vinodgopal, S. Hotchandani, P.V. Kamat, J. Phys. Chem. 97 (1993) 9040–9044.
[14] J. Luo, M. Hepel, Electrochim. Acta 46 (2001) 2913–2922.
[15] J. Krysa, J. Jirkovsky, J. Appl. Electrochem. 32 (2002) 591–596.
[16] T. An, Y. Xiong, G. Li, C. Zha, X. Zhu, J. Photochem. Photobiol. A: Chem. 152 (2002) 155–165.
[17] I.M. Butterfield, P.A. Christensen, A. Hamnett, K.E. Shaw, G.M. Walker, S.A. Walker, C.R. Howarth, J. Appl. Electrochem. 27 (1997) 385–395.
[18] F. Krämer, N. Mencke, The biology of the cat flea, control and prevention with imidacloprid in small animals, in: Flea Biology and Control, Springer–Verlag, Berlin, Heidelberg, New York, 2001.
[19] J. Doull, C.D. Klassen, M.O. Amdur (Eds.), Cassarett and Doull's Toxicology. The Basic Science of Poisons, 4th ed., Pergamon Press, Elmsford, New York, 1991.
[20] E. Valatka, Z. Kulesius, J. Appl. Electrochem. 37 (2006) 415–420.
[21] A.M. Braun, M. Maurette, E. Oliveros, Photochemical Technology, Wiley, New York, 1991.
[22] S. Roy Morrison, Electrochemistry at Semiconductors and Oxidized Metal Electrodes, Plenum Press, New York, 1980, p. 126.
[23] S. Licht, Semiconductor electrodes and photoelectrochemistry, in: A. Bard, M. Stratmann (Eds.), Encyclopedia of Electrochemistry, vol. 6, Wiley-VCH, 2002.
[24] J.F. Juliao, F. Decker, M. Abramovich, J. Electrochem. Soc. 127 (1980) 2264–2269.
[25] H.O. Finklea (Ed.), Semiconductor Electrodes, Elsevier, New York, 1988, p. 71.
[26] M. Neumann-Spallart, Chimia 61 (2007) 806–809.
[27] I. Mintsouli, N. Philippidis, I. Poulios, S. Sotiropoulos, J. Appl. Electrochem. 36 (2006) 463–474.
[28] A.J. Bard, J. Photochem. 10 (1979) 59–75.
[29] H. Gerisher, Electrochim. Acta 35 (1990) 1677–1699.
[30] C.S. Turchi, D.F. Ollis, J. Catal. 122 (1990) 178–192.

[31] J. Cunningham, G. Al-Sayyed, S. Srijaranai, Adsorption of model pollutants onto TiO_2 particles in relation to photoremedation of contaminated water, in: G. Helz, R. Zepp, D. Crosby (Eds.), Aquatic and Surface Photochemistry, Lewis Publishers, CRC Press, 1994, pp. 317–348, Chapter 22.
[32] R. Candal, W. Zeltner, M. Anderson, Environ. Sci. Technol. 34 (2000) 3443–3451.
[33] S. Tunesi, M.A. Anderson, J. Phys. Chem. 95 (1991) 3399–3405.
[34] J. Kesselman, N. Lewis, M. Hoffmann, Environ. Sci. Technol. 31 (1997) 2298–2302.
[35] V. Myamlin, Y. Pleskov, Electrochemistry of Semiconductors, Plenum Press, New York, 1967.
[36] S. Yang, Y. Liu, C. Sun, Appl. Catal. A: Gen. 301 (2006) 284–291.
[37] D.H. Kim, M.A. Anderson, J. Photochem. Photobiol. A: Chem. 94 (1996) 221–229.